The Henryk Niewodniczański
INSTITUTE OF NUCLEAR PHYSICS
Ul. Radzikowskiego 152, 31-342 Kraków, Poland.

www.ifj.edu.pl/reports/2000.html

Report No 1853/PL

Forward Wall Detector

A. Budzanowski, B. Czech, A. Siwek, I. Skwirczyńska and P. Staszel.

Abstract

The Forward Wall Detector is designed to identify projectile like fragments from heavy ion reactions at CELSIUS storage ring in Uppsala, Sweden. The FWD consists of 96 detection modules covering azimuthal angle from 3.9^o to 11.7^o with an efficiency of 81%. The detection module can be either of phoswich type (10mm fast plastic + 80mm CsI(Tl)) or standard ΔE-E telescope (750μm Si + 80mm CsI(Tl)). It is expected to have charge identification up to Z=18, mass resolution for H and He isotopes and energy resolution ~8%.

Kraków, November 2000

1. Introduction

Present-day experiments on high energy nucleus-nucleus collisions require detection of high multiplicity events. Energetic light particles at beam velocities are emitted mostly at forward angles. Therefore systems comprising several hundreds small single detectors located at forward direction are necessary. To disentangle between various reaction mechanisms e.g. compound nucleus emission, direct processes, transfer reactions, deep inelastic scattering coincidence measurements between particles emitted at all reaction angles are necessary. Charge identification, energy and angle of emission are usually required to reconstruct the mass, energy and angular momentum of the primary fragments.

The Forward Wall Detector (FWD) is a separate, stand-alone part of the CHICSi system[1)]. It is designed to determine charge and energy of projectile-like fragments (PLF) from heavy ion reactions in the beam energy range 50 – 450MeV/nucleon. A wide energy range required a careful design of a detection module which is described in section 2. Geometry and construction of the FWD are described in section 3. In section 4 an electronics required to operate the device is discussed. The identification capability achieved until now is given in section 5, followed by some conclusions.

2. The detection module

The identification of PLF's charge in a large dynamic range was the main factor which determined the FWD design. The basic detector module is a telescope based on the standard ΔE-E technique. Two types of telescopes with different ΔE detectors have been built:

- The phoswich detector consisted of 10mm fast plastic scintillator (BC408 – Bicron) with 80mm CsI(Tl) crystal (Amacrys-H, Charkhov)
- The 750μm (ΔE) silicon detector followed by 80mm CsI(Tl) crystal (Amacrys-H, Charkhov)

Four phoswich detectors placed at the same azimuthal angle are equipped with common thin (1.5mm) plastic scintillator (BC444 – Bicron) to decrease lower energy threshold. An identification of hydrogen and helium isotopes is possible by using either pulse shape discrimination method or a good quality silicon detector in front of CsI crystal. The actual energy limits for full PLF identification (charge, energy) in the phoswich module are shown in the Table 1.

	Energy minimum [MeV/n]	Energy maximum [MeV/n]
Proton	17	180
^{2}H	11	120
^{3}H	9	95
^{3}He	19	210
^{4}He	18	180
^{6}Li	21	230
^{7}Li	19	210
^{9}Be	22	255
^{11}B	25	300
^{12}C	30	350
^{14}N	32	390
^{16}O	35	420
^{20}Ne	39	490
^{24}Mg	43	550
^{28}Si	47	610
^{40}Ar	51	670

Table 1. The energy range of fully stooped particles in the phoswich module

The CsI(Tl) crystals and the fast plastic scintillators are tapered with trapezoidal shapes. The cross section through a detection module is shown in fig. 1.

Each CsI(Tl) is glued to the Plexiglas light guide with Bicron BC-600 optical cement. A fast plastic scintillator is optically connected to CsI(Tl) crystal with Bicron BC-630 optical grease. There is ~1mm gap between the light guide and the photomultiplier face. All CsI(Tl)/phoswich detectors are coupled to R7400U Hamamatsu photomultiplier with a photocatode diameter of 8mm. The additional thin plastic scintillator is coupled by the Plexiglas light guide to R6095 Hamamatsu photomultiplier with a photocatode diameter of 28mm.

Faces of all detectors are covered by an aluminized Mylar foil of 50µm thickness. All scintillators and light guides are wrapped with white 75µm Teflon tape surrounded by 20µm aluminium foil. To maximize packing there is no housing around the scintillators.

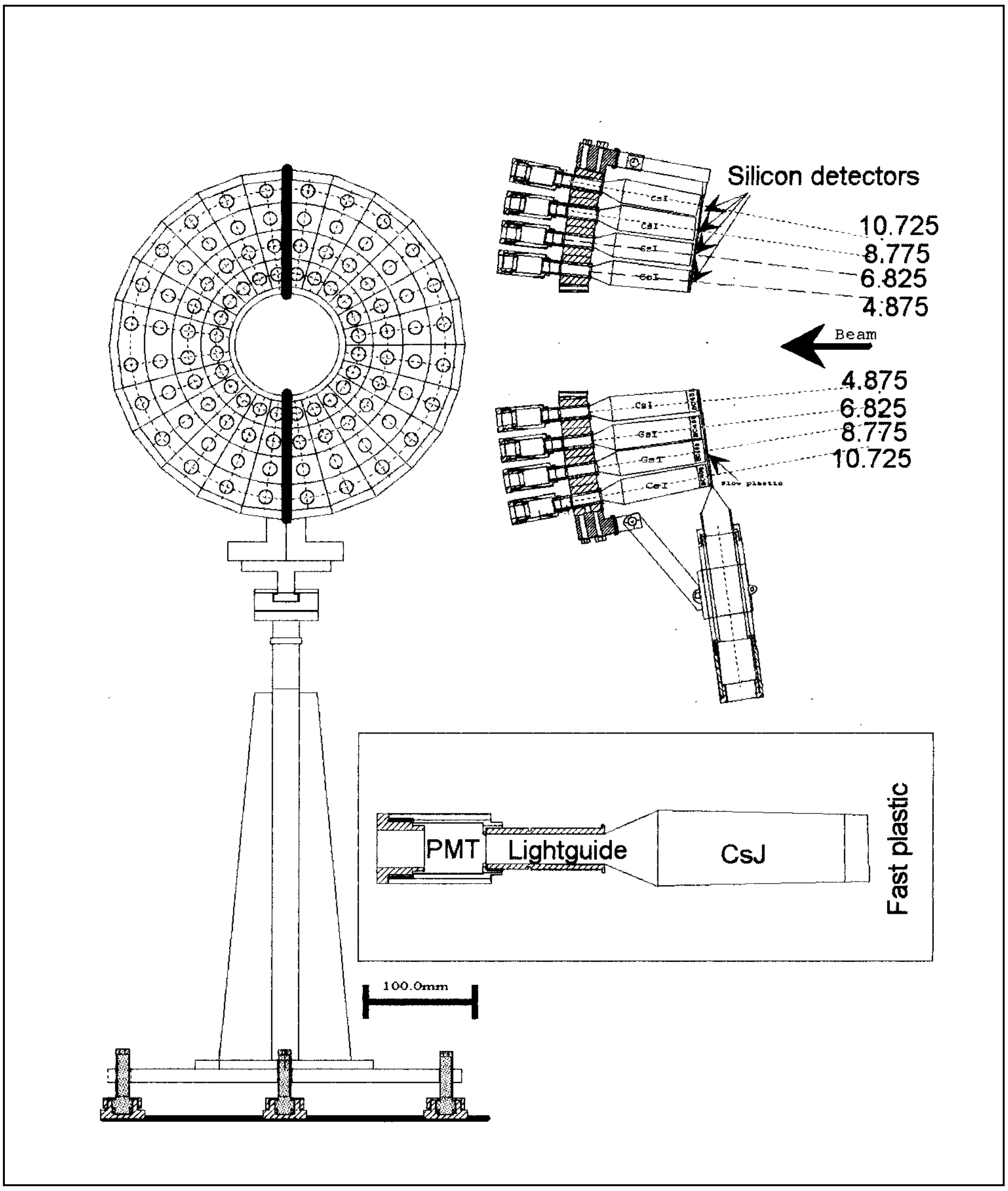

Fig. 1. Forward Wall Detector and Detection Module.

3. Geometry and construction of Forward Wall Detector

The numerical simulation by Monte Carlo techniques of the interaction of particles with complex detectors, has proved to be a practical way of handling the design of large experimental setups. We have used GEANT3 (version3.21)[2] and results of the CHIMERA[3]+GEMINI[4] codes to optimise the FWD geometry in order to achieve following goals:

- suppression of the cross talk effect between adjacent detection modules,
- reduction of multiple hits probability,
- optimization of scintillator geometrical shape for the best light collection and consequently the best energy and time resolution of each module
- Counting rate balance for each ring.

The total thickness of CsI scintillator is a compromise between the requirement of minimizing a nuclear interaction probability and maximizing a stopping energy. The maximum expected energy of PLF's is defined by the highest beam energy available, which at the moment is 450MeV/n.

Randomly distributed bunch of protons, alpha particles and ^{12}C coming from the interaction region (11mm thick gas-jet target with 5.5mm beam diameter) entered the FWD detection module placed 764 mm away. The fraction of particles removed from the crystal by lateral escape was determined for each ring. For 80mm thick CsI crystal of the 1st ring the maximum of 35% nuclear interaction probability is reached for barely stopped protons of 180MeV. This fraction decreases for the other rings and is lower than 4% for the fourth

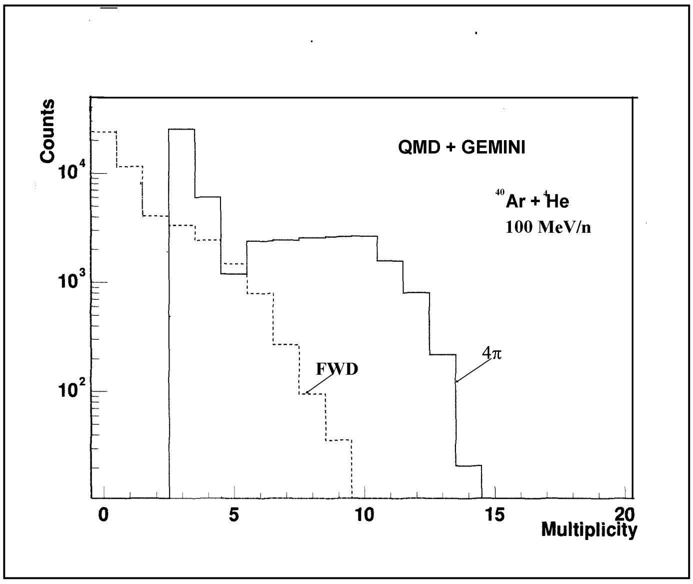

Fig. 2. The total and registered multiplicity for $^{40}Ar+^{4}He$ reaction at 100MeV/n calculated with CHIMERA+GEMINI.

ring. For fragments with Z > 3 the interaction probability is much lower than for protons, since their range diminishes more rapidly than the reaction cross section increases.

The Monte Carlo simulations has been made using the QMD code CHIMERA[3)] and statistical evaporation afterburner GEMINI[4)]. A multihit probability for ^{40}Ar+^{84}Kr reaction at 100MeV/nucleon was calculated to be less than 4% of all particles registered in the FWD. The total and detected by the FWD multiplicity from ^{40}Ar+^{4}He at 100MeV/nucleon are shown on fig. 2. Angular distributions of the elements with charge 1 to 12, from the same reaction are shown on fig. 3. For this kind of reverse kinematics the FWD is a very efficient detector and registers more than 30% of all emitted particles. Number of reaction products emitted into the beam tube, active area of FWD, places between phoswiches and outside of the wall are shown by intensity plots on fig. 4.

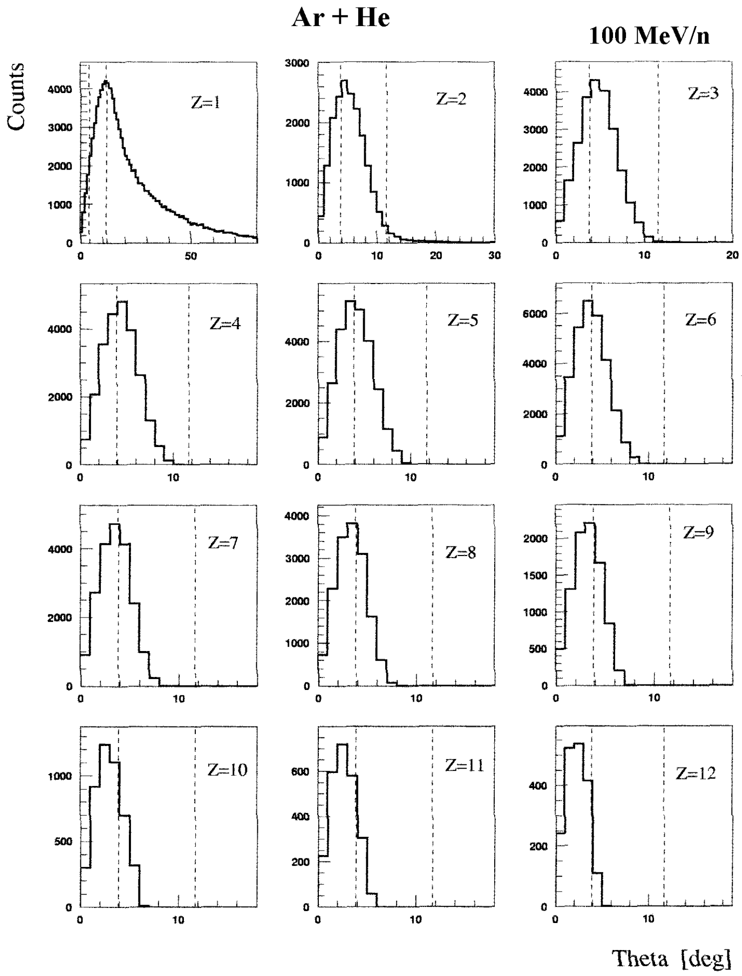

Fig. 3. The angular distributionof PLF's from ^{40}Ar+^{4}He at 100MeV/n reaction calculated with CHIMERA+GEMINI. The dashed line show the angular range of FWD.

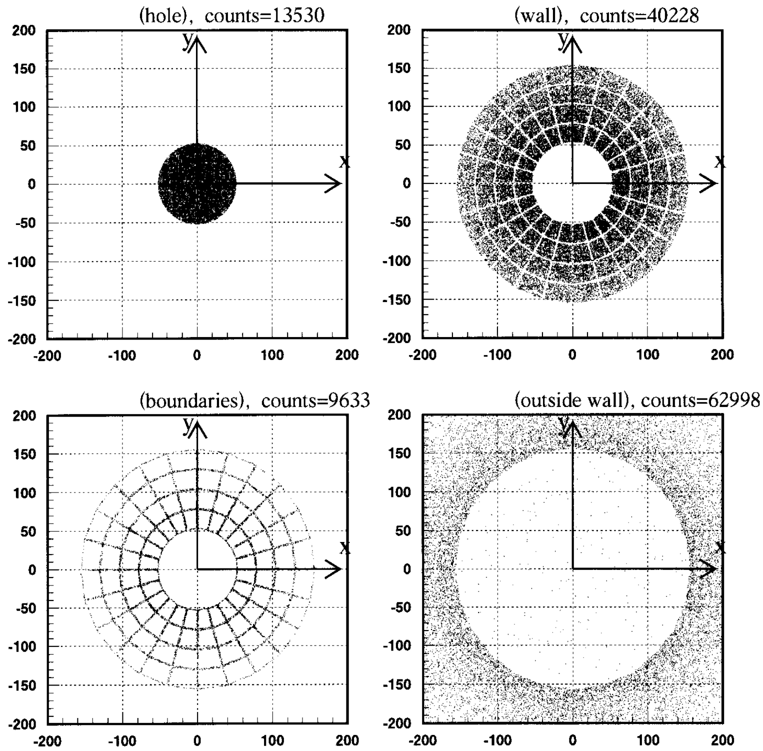

Fig. 4. The distribution of registered particles in different parts of full sphere.

After all the simulations described to above the following geometry was chosen:
four rings of 10mm plastic + 80mm CsI(Tl)with constant $\Delta\varphi$ =15° and constant $\Delta\theta$ =1.95° supplemented by 1.5mm plastic common for radial section of four phoswich detectors. The solid angles and the surfaces of the detector faces are 7.1×10^{-4}sr ($412.7mm^2$), 10.1×10^{-4}sr ($588.2mm^2$), 13.2×10^{-4}sr ($767.7mm^2$), 16.2×10^{-4}sr ($943.2mm^2$) for each ring, respectively. The use of silicon detectors instead of fast plastic scintillators improves mass resolution as compared to pulse shape discrimination method. Additionally, it allows avoiding the complicated and time consuming energy calibration of the large number of CsI scintillators.

The FWD covers the forward angular range of 3.9°-11.7°, filling the 0.17π of whole sphere with geometrical efficiency of 81%. In its final version FWD will consist of 96 closely packed detection modules arranged in 4 concentric rings. The detectors are placed 764mm away from target, outside of the scattering chamber. The mechanical structure support the sphere and allows its alignment along the beam axis (fig. 5), the details of FWD construction are shown on Fig.1.

Half of the FWD will be ready by mid of 2001 and will consist of 24 phoswiches with six thin (1.5mm) plastic scintillators and 24 Si+CsI(Tl) modules.

Fig5. The mechanical support of FWD

4. Electronics

A schematic diagram for the electronics controlling the FWD during an experiment is shown in fig. 6.

The plastic scintillator pulses have a 3ns decay time. The CsI(Tl) pulses have two decay components. The first component has a decay time of 0.3-1.0μs which depends on the particle type. The second component has a decay time of 7μs which is insensitive to the type of the detected particle.

The PMT signal from phoswich module is split linearly into two outputs. One of the signals is differentiated and split into two parts: trigger and ΔE signal. The other one is used to create a linear E signal which is passively split into two equal signals. They are attenuated by factors 10 and 4 for the slow and the long components of the CsI(Tl), respectively. The fast, slow and long signals are delayed by 200ns and are subsequently integrated by QDC with 25, 300 and 2000ns gates.

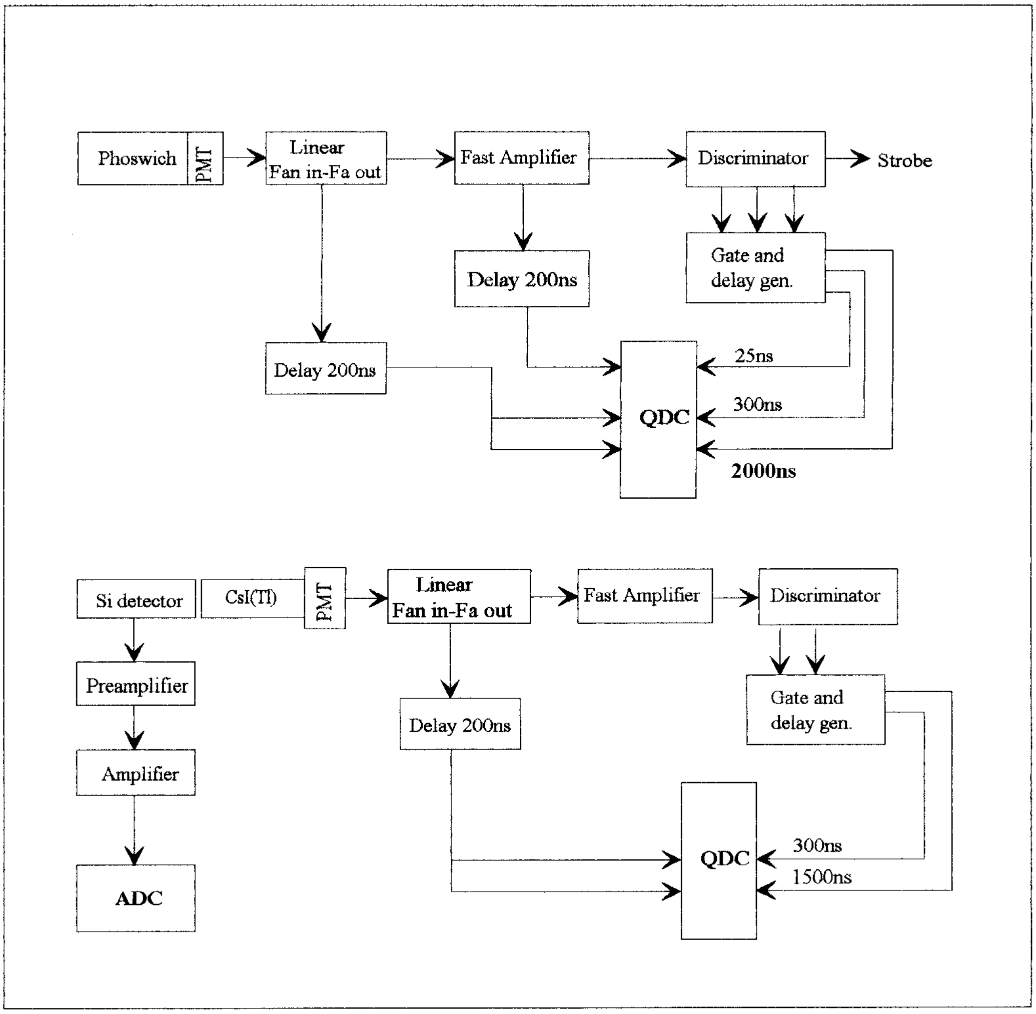

Fig. 6. Schematic diagram of electronics

In order to obtain the desired dynamical range of detected energies, the main amplifiers were provided with two processing channels, having gains differing by a factor of 5, coupled to two different QDCs.

The signal from the silicon detector is sent to preamplifier and next to slow and fast amplifiers. The energy signal is provided by ADC.

5. Particle identification

Some test runs of the FWD detection module have been performed at TSL with 200MeV/nucleon ^{20}Ne beam on ^{131}Xe target and 300MeV/nucleon ^{16}O beam on ^{131}Xe and ^{40}Ar targets.

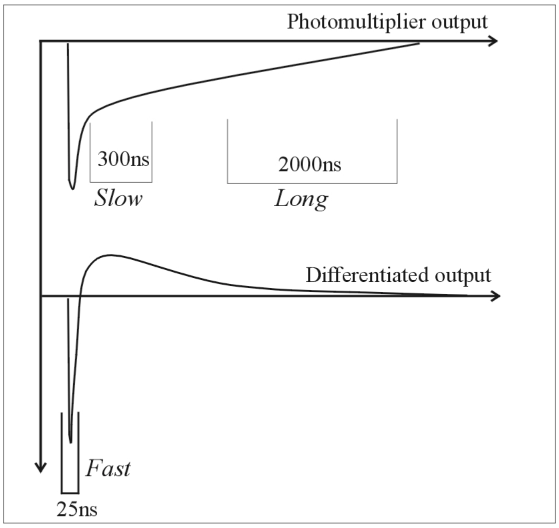

Fig. 7. The phoshwich signals with the definition of fast, slow and long gates.

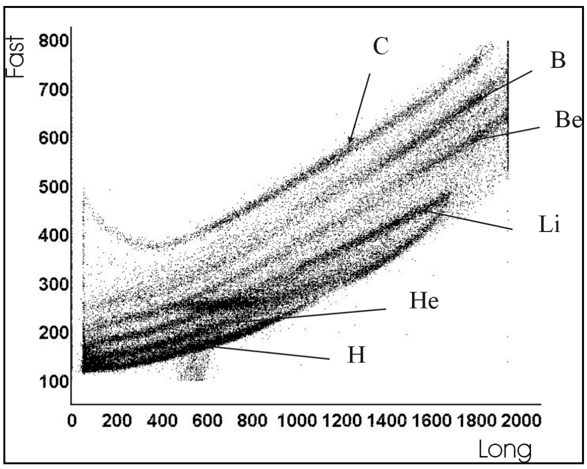

Fig. 8. Scatter plot of the fast vs. long component for ^{16}O+^{131}Xe at 300MeV/n reaction.

Particle identification by phoswich detectors can be done from two types of scatter plots, the long vs. slow and the fast vs. long component (fig. 7). In figs. 8, 9 two- dimensional spectra from FWD phoswich centred at θ=5.5° for $^{16}O+^{131}Xe$ reaction at 300MeV/n can be seen. Charge separation up to Z=6 was achieved however hydrogen and helium isotopes were not resolved.

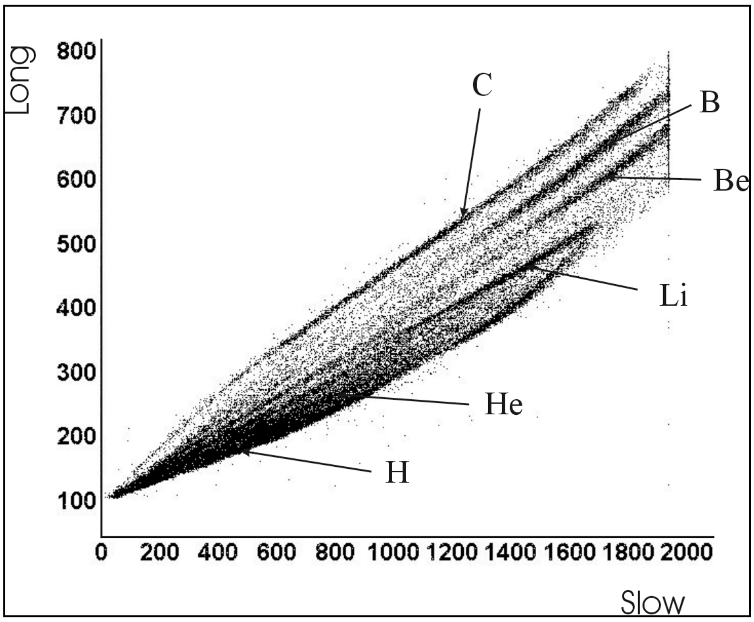

Fig.9. Scatter plot of the long vs. slow component for $^{16}O+^{131}Xe$ at 300MeV/n reaction.

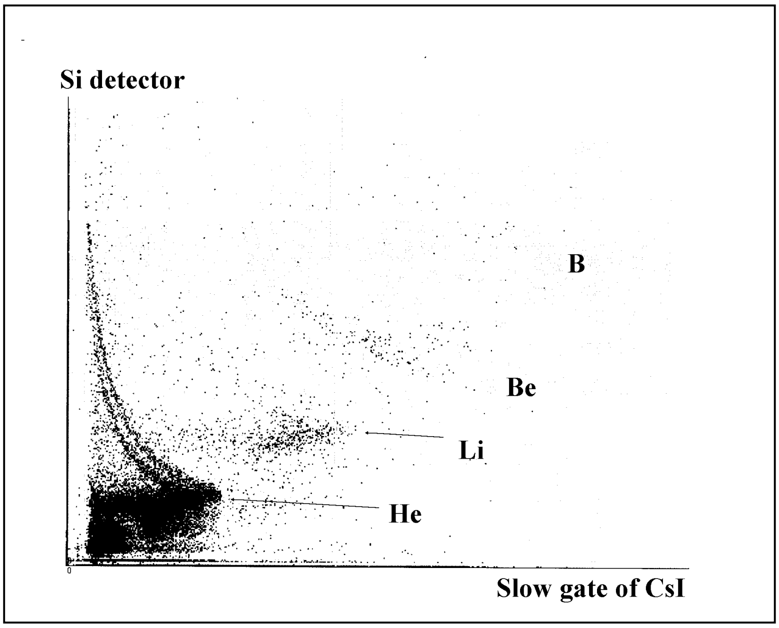

Fig. 10. Scatter plot of the silicon detector vs. slow component of CsI for $^{16}O+^{40}Ar$ reaction at 300 MeV/n.

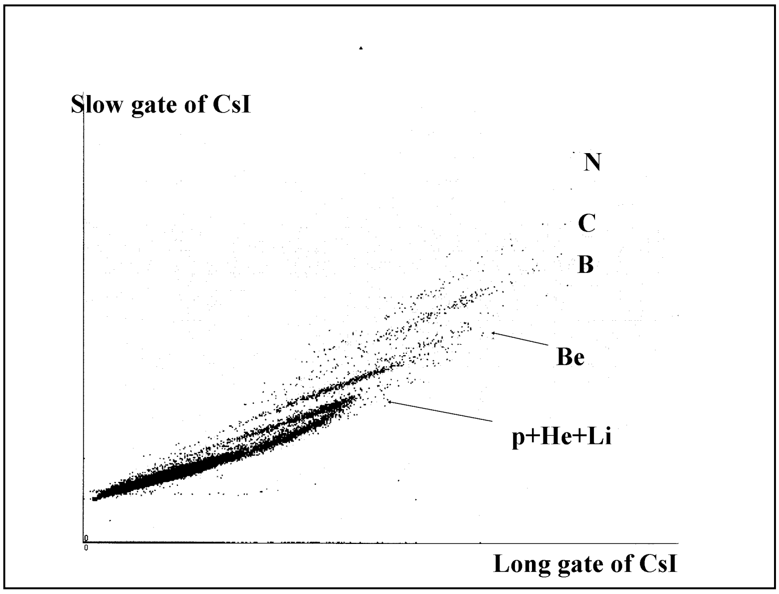

Fig. 11. Scatter plot of the long vs. slow component for reaction $^{16}O+^{40}Ar$ reaction at 300 MeV/n.

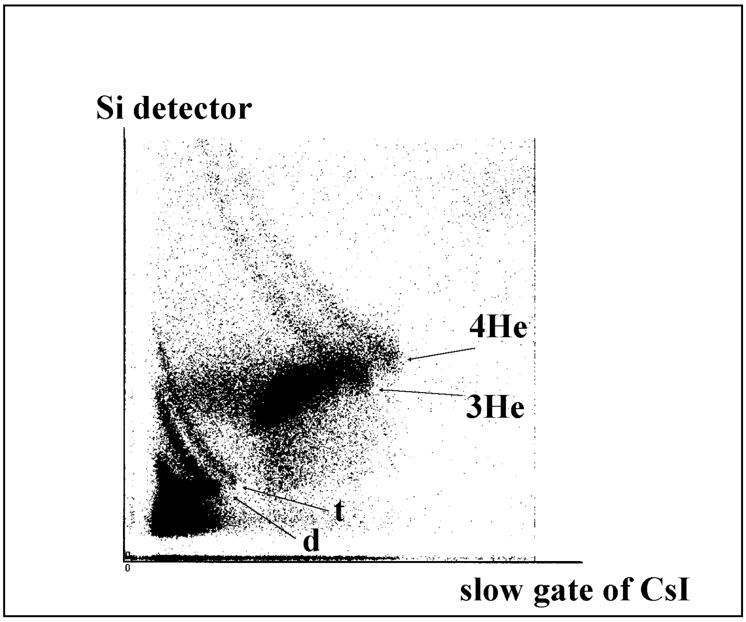

Fig. 12. The same as in fig. 9, but with higher gain.

Figs 10, 11, 12 show the same two dimensional spectra for telescope silicon detector + CsI(Tl) scintillator. The mass resolution for H and He isotopes is satisfactory.

6. Summary

In summary, multidetector system for PLF identification, which can operate in conjunction with the CHICSi detector has been constructed and is being manufactured. It has good charge resolution (tested up to Z=7), mass resolution for light isotopes and more than 30% efficiency for reverse kinematics. This device significantly increases detection capabilities of CHICSi detector and enables more comprehensive and exclusive studies of reaction mechanisms. The FWD can also be used as a stand alone detector especially in the case of reverse kinematics.

The research was supported by Grant No 2P03B 126 15 from the Polish State Committee for Scientific Research.

7. References:

1. A.Siwek and CHIC Collaboration, Nucl.Phys. A654(1999)2695
2. R.Brun, F.Bruyant, M.Maire, A.C.McPherson and P.Zanarini, GEANT3 User Guide
3. J.Łukasik et al., Phys.Lett. B318(1993)419
4. R.J.Charity et al., Nucl.Phys. A483(1988)371